Electronic Supplementary Material (ESI) for Environmental Science: Advances.

Supporting Information:

A simple microscopy approach quantifies biomineralized CO2 in *Coccolithus braarudii* – a calcifying marine phytoplankton

Toby Morton-Collings,[a] Minjun Yang,[a] Christopher Batchelor-McAuley,[a] Samuel Barton,[b] Rosalind E.M. Rickaby,[b] Heather A. Bouman,[b] Richard G. Compton[a*]

[a] Mr T. Morton-Collings, Dr. M. Yang, and Prof. R. G. Compton
Physical and Theoretical Chemistry Laboratory, Department of Chemistry
University of Oxford,
South Parks Road, Oxford, Great Britain
E-mail: Richard.Compton@chem.ox.ac.uk
[b] Dr. S. Barton, Prof. R. E. M. Rickaby and Prof. H. A. Bouman
Department of Earth Sciences,
University of Oxford,
South Parks Road, Oxford, Great Britain

Section 1: Hypothetical Mass-transport limited flux

In this section, we derive expressions to calculate the maximum amount of $CaCO_3$ that can be dissolved from a calcite particle on a plate if the overall dissolution reaction is limited by mass-transport. We first derive expressions for a cuboid particle on a plate before moving to a spherical particle on a plate.

Cuboid on a plate

The steady-state mass-transport flux (J_{MT}) to a cuboid on a plate, with the height of the cube equal to 1/10 its side length (L), as shown in Equation 2 in the main manuscript, was reported by Wong *et. al.*[1]

$$J_{MT}(\text{mol s}^{-1}) = \frac{\text{dmoles}}{\text{dt}} = \frac{11.65 D \Delta c L}{4} \qquad \textit{Equation S1}$$

where, as mentioned in the main text, D is the geometric average diffusion coefficient of Ca^{2+} and CO_3^{2-}, Δc is the difference in concentration at the interface at chemical equilibrium and the bulk ($c_{eq} - c_{bulk}$). The factor of 11.65 appearing in Equation S1 was

was obtained via finite difference numerical simulation in the work by Wong *et.al.*[1] Equation S1 can be rewritten to describe the rate of change of the side-length of the cube, $\frac{dL}{dt}$

$$\frac{J_{MT}Mw}{S_f\rho_{CaCO_3}A} = \frac{mol}{s} * \frac{1}{m^2} * \frac{g}{mol} * \frac{m^3}{g} = -2\frac{dL}{dt}\ (m\ s^{-1}) \qquad \textit{Equation S2}$$

where A is the area of the stubby cuboid exposed to the solution ($1.4L^2$), Mw is the weight of $CaCO_3$ (101 g mol^{-1}), ρ_{CaCO_3} is the density of calcite (2.71 x 10^6 g m^{-3}) and the factor S_f accounts for the fact that coccoliths, modelled as a stubby cuboid herein, is less dense compared to a pure calcite (ρ_{CaCO_3}) of the same geometric volume. An value of S_f of 0.6 was derived using the recommended species-specific shape-factor reported by Young *et. al.*[2] where he expressed the actual volume of *Coccolithus pelagicus* coccoliths to the *cube* of its length: volume $(V) = 0.06l^3$. Using this relationship, for a stubby cuboid where the height (h) is 1/10th of its side lengths ($L = 10h$), the actual calcite volume to its geometric volume is obtained, $S_f = 0.06 * (10h * L^2)/hL^2 = 0.6$. The factor of two appearing in Equation S2 is due to the fact that dissolution occurs at all faces of the cuboid exposed to the solution, resulting in an equal rate of shrinkage of cube side-length from *both* sides. The rate of change in the projection area of the cuboid is obtained by integrating Equation S2

$$\int_0^t \frac{dL}{dt} = \int_0^t -\frac{1.04D\Delta cMw}{\rho_{CaCO_3}L} \qquad \textit{Equation S3}$$

Rearranging following by integration gives

$$\int_0^t LdL = -\frac{1.04D\Delta cMw}{\rho_{CaCO_3}}\int_0^t dt \qquad \textit{Equation S4}$$

$$(L(t)^2 - L(t=0)) = -\frac{2.08D\Delta cMw}{\rho_{CaCO_3}}t \qquad \textit{Equation S5}$$

Differentiating Equation S5 with respect to the projection area of the cuboid with time gives

$$\frac{d\text{projection area}}{dt} = \frac{dL(t)^2}{dt} = -\frac{2.08D\Delta cMw}{\rho_{CaCO_3}} \qquad \textit{Equation S6}$$

Note that in Equation S6, the density and molecular weight of calcite remains constant with small changes in temperature. The thermodynamics and diffusion coefficients, however, are functions of temperature and salinity, as summarised in a review by Millero.[3] Using literature-reported values, the solubility constants and diffusion coefficients can be calculated in DI water for different temperatures.[4] At 291 K, the calcite solubility is 0.114 mM and the geometric mean of the calcium and carbonate diffusion coefficient is 7.25 x 10^{-10} m^2 s^{-1}.[4] Similarly, at 298 K, the calcite solubility and the geometric mean of the calcium and carbonate diffusion coefficient is higher with values of 0.123 mM and 8.70 x 10^{-10} m^2 s^{-1}, respectively.[4] Substituting the above values into Equation S6 facilitates the generation of solid lines shown in Figure 3.

Sphere on a plate

The rate of change in the projection area of a calcite sphere on a plate dissolving at the mass-transport limit can be derived much as done above for the cuboid. The steady-state mass-transport flux (J_{MT}) to a sphere on a plate is[5]

$$J_{MT}(\text{mol s}^{-1}) = \frac{d\text{moles}}{dt} = \ln(2)4\pi D\Delta cr \qquad \textit{Equation S7}$$

where r is the radius of the sphere, D is the diffusion coefficient and Δc is the change in concentration from bulk to a saturated solution. Dividing through by the surface area of a sphere ($area = 4\pi r^2$) gives:

$$j\left(\text{mol m}^{-2}\text{ s}^{-1}\right) = \frac{D\Delta c \ln 2}{r} \qquad \textit{Equation S8}$$

Analogous to the cuboid derivation, Equation S8 can be expressed in terms of the rate of change of the spherical radius

$$\frac{dr}{dt}\left(\text{ms}^{-1}\right) = -\frac{jM_w}{\rho_{CaCO_3}} = -\frac{D\Delta c \ln 2 M_w}{r\rho_{CaCO_3} f} \qquad \textit{Equation S9}$$

f is introduced herein as the 'fill factor' which accounts for the gaps present in the calcite shell as the structure of the latter is constructed via "interlocking" coccoliths. In this work, we use a reported fill factor of 0.60 from previous work.[6] Equation S9 can be rearranged follow by integration to give the projected area of the calcite sphere

$$\int r\, dr = -\frac{D\Delta c \ln 2 M_w}{\rho_{CaCO_3} f}\int dt \qquad \textit{Equation S10}$$

$$r(t)^2 - r_i^2 = -\frac{2D\Delta c \ln 2 M_w}{\rho_{CaCO_3} f} t \qquad \textit{Equation S11}$$

Multiplying both sides by π gives:

$$\pi r(t)^2 = \pi r_i^2 - \frac{2\pi D\Delta c \ln 2 M_w}{\rho_{CaCO_3} f} t \qquad \textit{Equation S12}$$

Differentiation with respect to time gives:

$$\frac{dArea}{dt}\left(\text{m}^2\text{s}^{-1}\right) = -\frac{2\pi D\Delta c \ln 2 M_w}{\rho_{CaCO_3} f} \qquad \textit{Equation S13}$$

Equation S13 was used to estimate the rate of change in the projection area of *C. braarudii* coccosphere if it were to dissolve at the mass-transport limit. The results are shown in Figure 5b).

Section 2: Coccolith thickness and reconstruction images

Figure S1 shows an SEM image of *C. braarudii* coccoliths allowing its thickness to be qualitatively measured. The distance between the bottom to the top of a coccolith is approximately 1.6 μm, which is approximately 1/10 compared to the coccolith lengths studied in the main text, shown in Figure 4.

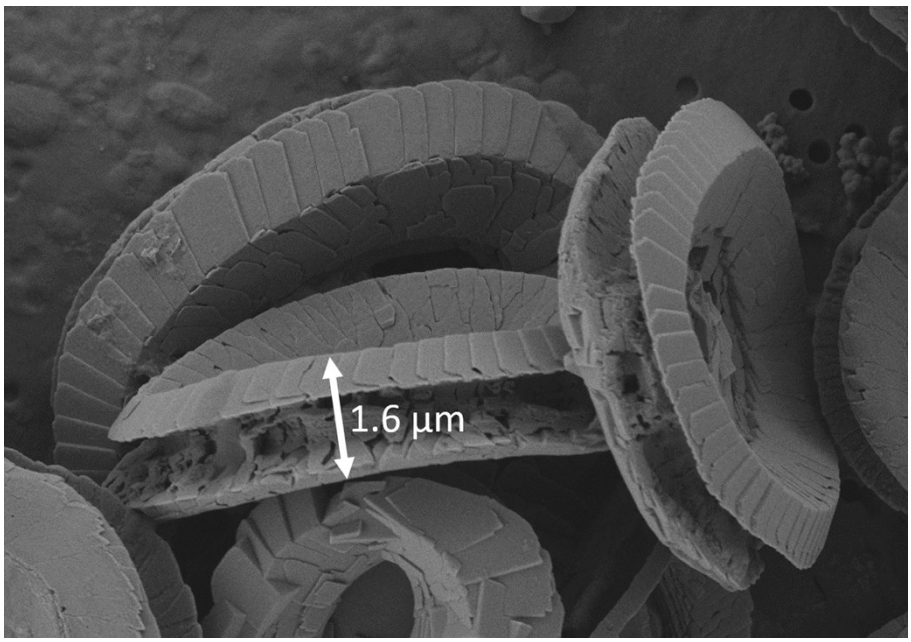

Figure S1. SEM image of C. braarudii coccoliths.

Figure S2 shows two complementary 3-D reconstructed images of *C. braarudii* coccoliths along with their corresponding optical image prior to the start of auto-dissolution. The reconstructed coccolith image shown in Figure S2 a) suffered from slightly distortion because of a slight shift in the coccolith position during the auto-dissolution. This does not affect the calculated coccolith volume as its calculation requires summation over the entire reconstructed image. Note that, theoretically, the volume of the reconstructed coccolith is independent to the orientation of the coccolith (upside down or vice versa).

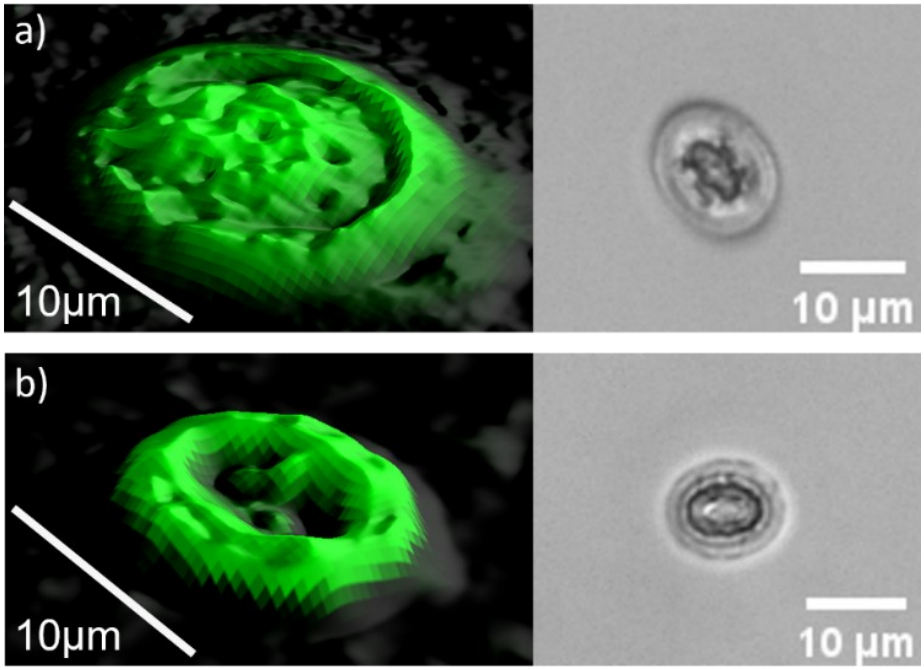

Figure S2. Two additional examples of 3D reconstructed images of coccolith and its corresponding optical image prior to dissolution in DI water. Reconstructed C. braarudii coccoliths have heights in the range of 1 - 2µm. Scale bars = 10 µm.

Section 3: Effect of ionic strength on living coccolithophores

Figure S3 show images of intact *C. braarudii* coccolithophores obtained using a) scanning electron and b) optical microscopes. In the SEM image, it is clear that the coccosphere shell is comprised of 10-20 "interlocking" coccoliths.[7] Figure S4 shows the projection area of a living *C. braarudii* coccolithophore as a function of time following immersion in deionised water saturated with respect to $CaCO_3$. Over a time period of 1.5 hours, a steady increase in the projection area of the *C. braarudii* coccolithophore is seen. After 18 hours of immersion, images shown in Figure S4 b), 33 and 45% increases in the projection area of two *C. braarudii* coccolithophore individuals were measured. It is inferred that the increase in coccolithophore size as a function of time is due to the increase in osmotic pressure of the underlying cell when transferred from its seawater mimicking culture medium to that of lower ionic strength.

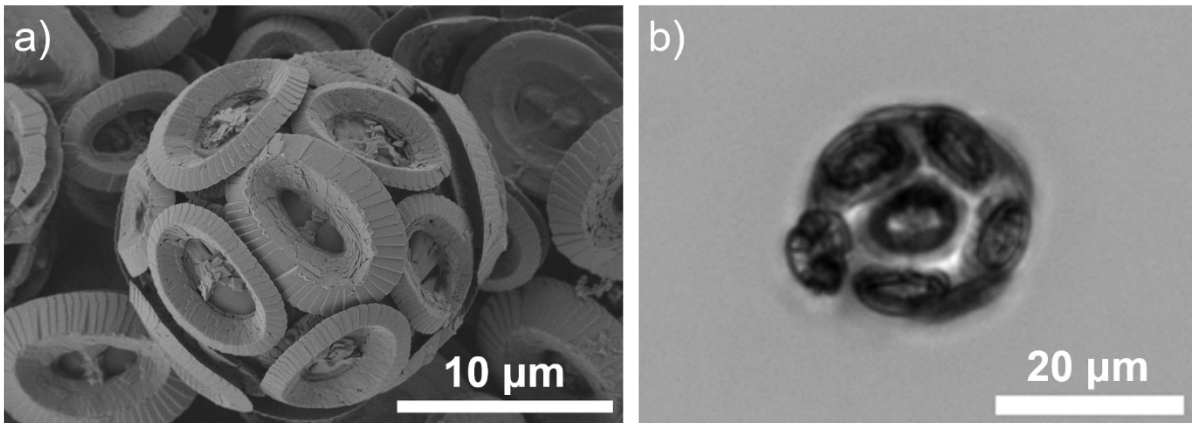

Figure S3. Representative images of C. braarudii coccosphere imaged via a) a scanning electron microscope and b) an optical microscope: 20x objective lens and bright-field illumination.

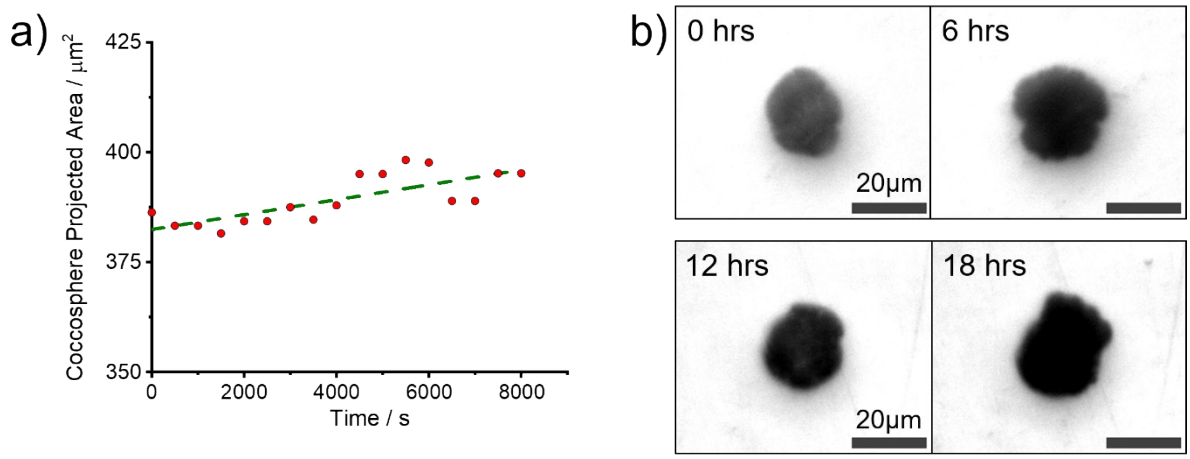

Figure S4. a) 2D projection area of a coccolithophore when placed in DI solution saturated with respect to $CaCO_3$. A slope of $1.7x10^{-15}$ m^2s^{-1} was fitted to the experimental data. b) optical images of the same coccolithophore over 18 hours of immersion.

Figure S5 shows the projection area of *C. braarudii* coccolithophores transferred to aqueous solutions saturated with respect to $CaCO_3$ *and* containing a) no NaCl, b) 0.35M NaCl and c) 0.7M NaCl. Under the same conditions, the experimental reproducibility between each coccolithophore individual differs slightly. However, across all conditions, generally, the larger the coccolithophore (i.e. larger the projection area) the longer it requires for the shell to dissolve completely.

Interestingly, at 0.7M NaCl, where the ionic strength is equivalent to that of seawater, the coccosphere projection area remains constant for ca. 1000s before a rapid drop in its area as a result of the falling apart of the coccosphere leading to the appearance of shrapnel (see Coccosphere_0.7M_NaCl.avi). Figure S6 plots the average time required for particulate "shrapnel" to appear under different concentrations of NaCl since the initial immersion. At higher salt conditions, the quicker appears the "shrapnel" arising from the destruction of the coccosphere. This is expected as the rate of calcite dissolution in undersaturated solution increases with the ionic strength of the solution.

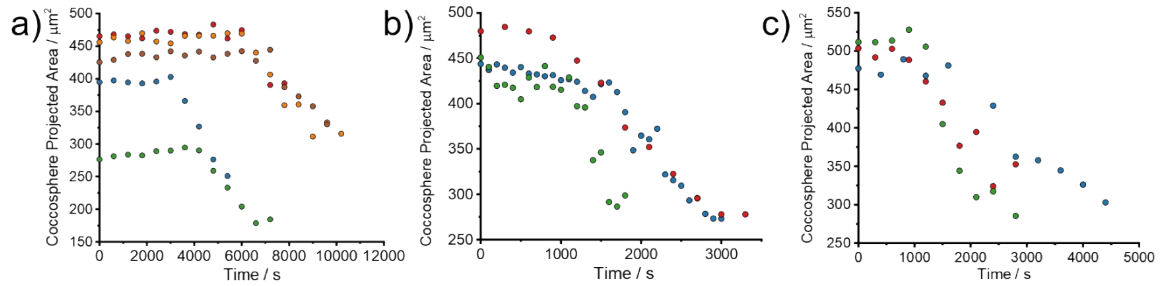

Figure S5. Plots of the 2D projection area of C. braarudii coccospheres as a function of time in different ionic strength aqueous solutions. a) De-ionised water. b) 0.35M NaCl(aq). c) 0.7M NaCl(aq). Different coccolithophore in each chart is represented by individual colours.

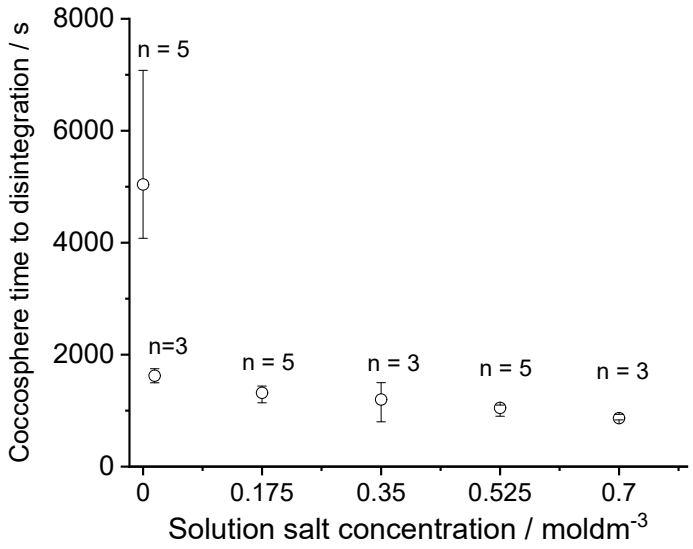

Figure S6. A plot of the average time required for shrapnel to appear in different salt (NaCl) concentrations.

Section 4: Extra Figures

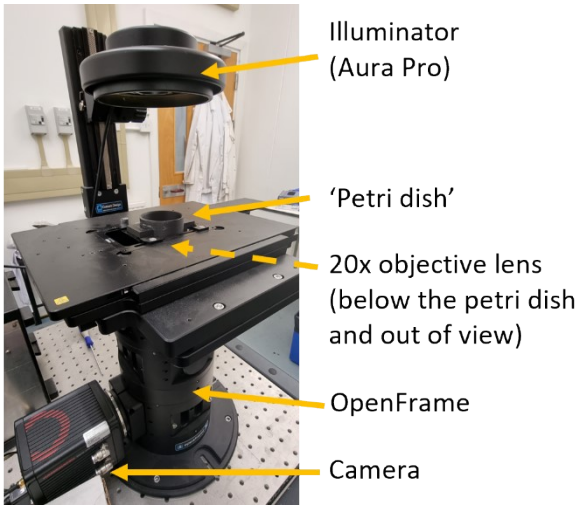

Figure S7. Picture of the openFrame microscope used to monitor single coccolith and coccolithophore dissolution in DI water.

References

1. R. Wong, C. Batchelor-McAuley, M. Yang and R. G. Compton, *Journal of Electroanalytical Chemistry*, 2021, **903**, 115818.
2. J. R. Young, S. A. Davis, P. R. Bown and S. Mann, *Journal of structural biology*, 1999, **126**, 195-215.
3. F. J. Millero, *Chemical Reviews*, 2007, **107**, 308-341.
4. X. Fan, C. Batchelor-McAuley, M. Yang and R. G. Compton, *ACS Measurement Science Au*, 2022.
5. P. Bobbert, M. Wind and J. Vlieger, *Physica A: Statistical Mechanics and its Applications*, 1987, **141**, 58-72.
6. X. Fan, C. Batchelor-McAuley, M. Yang, S. Barton, R. E. Rickaby, H. A. Bouman and R. G. Compton, *Analytical Chemistry*, 2022.
7. T. Beuvier, I. Probert, L. Beaufort, B. Suchéras-Marx, Y. Chushkin, F. Zontone and A. Gibaud, *Nature Communications*, 2019, **10**, 1-8.